14B.6 **PARAMETERIZED CONVECTIVE MOMENTUM ADJUSTMENT**

Gary M. Lackmann
Kelly M. Mahoney
Matthew D. Parker
North Carolina State University, Raleigh, North Carolina

1. INTRODUCTION

Convection is known to alter distributions of temperature, moisture, and momentum. In numerical models running with a grid length in excess of ~4 km, convective processes are generally parameterized. Some numerical weather prediction (NWP) models are now being run with sufficiently small grid length to represent convection explicitly (EC), but for many applications convective parameterization (CP) is still required. Global models, many ensemble forecasting systems, and climate models will all continue to require CP schemes for the near-term future.

While there is variability in the design of modern CP schemes, parameterization techniques for temperature and moisture adjustment are relatively straightforward compared to the adjustment of momentum. Current treatments of convective momentum transport (CMT) range from complete neglect to inclusion with account for mesoscale pressure forces, but a universal strategy has not been developed. The importance of the CMT process has been demonstrated for organized convection (e.g., Moncrieff 1981; LeMone 1983; Flatau and Stevens 1987; Wu and Yanai 1994; Mechem et al. 2008; Mahoney et al. 2009). Accounting for CMT in general circulation models (GCMs) has been shown to be important for simulation of the ITCZ, ENSO, and other tropical circulation systems (e.g., Zhang and McFarlane 1995; Mapes and Wu 2001; Wu et al. 2003; Kim et al. 2008).

The CMT process has received somewhat less attention in limited-area mesoscale models. However, Kershaw and Gregory (1997), Gregory et al. (1997), Grubisic and Moncrieff (2000), Han and Pan (2005), Moncrieff and Liu (2006) and others have emphasized the importance of CMT parameterization in NWP. In the highly popular Weather Research and Forecasting (WRF) model, none of the available CP scheme currently pass momentum tendencies to the solver (as of version 3.2.1 of the WRF-ARW). Evidently, version 3.3 of this model will include some CP schemes that do adjust momentum.

The climate modeling community has done much to address the CMT issue, although some GCMs omit this process (Kim et al. 2008). These studies emphasize the importance of including an account of the mesoscale pressure field for organized convection (e.g., Gregory et al. 1997, Wu et al. 2003). Complications arise because this aspect varies with the structure and organization of the convective system (Wu and Yanai 1994). Furthermore, the grid lengths in GCMs are such that there is little or no representation of the actual convective system resolved on the grid scale. How does the CMT parameterization problem change for mesoscale models running with grid lengths that partially resolve organized convection but still require CP?

Many WRF applications involve high-resolution EC model runs; however, even such simulations often utilize CP on the coarser outer domains of nested EC domains. The purpose of this work is to explore the consequences of CMT omission in WRF for simulations of idealized convective systems at grid lengths on the order of 12 km. Organized convection includes a grid-scale signature at this resolution. Here, a version of the WRF model is modified to pass momentum tendencies from the Kain-Fritsch (KF) CP scheme to the solver. We compare experiments with the momentum adjustment version of KF (CMT) with those using the standard KF scheme (NOCMT). These 12-km runs are compared to higher resolution EC simulations of the same convective system with 1.3-km grid spacing.

+ *Corresponding author address:* Dr. Gary M. Lackmann, North Carolina State University, Dept. of Marine, Earth and Atmospheric Sciences, Raleigh, NC 27695. E-mail: gary@ncsu.edu.

2. METHODS

2.1. Convective momentum adjustment

The KF CP scheme is designed for use in relatively high resolution simulations, with grid length between 10 and 40 km. This scheme is based upon the assumption that convection will eliminate convective available potential energy (CAPE) within a time period that is related to the advective time scale. This scheme computes pressure-based updraft and downdraft mass fluxes (ω_u and ω_d, respectively) as well as entrainment and detrainment rates ε and δ. Thus, the potential temperature and specific humidity profiles are adjusted when the scheme is active via weighted redistribution of grid-scale quantities. Because the horizontal wind components experience accelerations due to changes in both the storm-scale and environmental pressure gradients with height, the representation of CMA is relatively complex. However, the approach of Kain and Fritsch (1990), following Fritsch and Chappel (1980a), is based on the basic premise that momentum is conserved in convective updrafts; this suggests the tendency equations (1) and (2) for changes in the zonal and meridional wind components due to convection

$$\left(\frac{\Delta \bar{u}}{\Delta t}\right)_{conv} \sim \frac{1}{\Delta p}\Big[\left(\omega_{u2}+\omega_{d2}\right)\bar{u}_2-\left(\omega_{u1}+\omega_{d1}\right)\bar{u}_1+ \left(\varepsilon_u+\varepsilon_d\right)\bar{u}_m-\delta_u u_{um}-\delta_d u_{dm}\Big], \quad (1)$$

$$\left(\frac{\Delta \bar{v}}{\Delta t}\right)_{conv} \sim \frac{1}{\Delta p}\Big[\left(\omega_{u2}+\omega_{d2}\right)\bar{v}_2-\left(\omega_{u1}+\omega_{d1}\right)\bar{v}_1+ \left(\varepsilon_u+\varepsilon_d\right)\bar{v}_m-\delta_u v_{um}-\delta_d v_{dm}\Big]. \quad (2)$$

Overbars denote grid-scale values, and subscripts 1 and 2 indicate the grid level beneath and above the level for which the momentum tendency is being computed, respectively. Entrainment and detrainment terms are explicitly included. For details on the derivation of (1) and (2), see Kain and Fritsch (1990) and Fritsch and Chapell (1980a,b).

Addition of momentum tendencies to the WRF model involved the modification of several routines, the details of which are not discussed here. However, the primary alterations were made to the program module_cu_kfeta.F, including the addition of (1) and (2) to that routine.

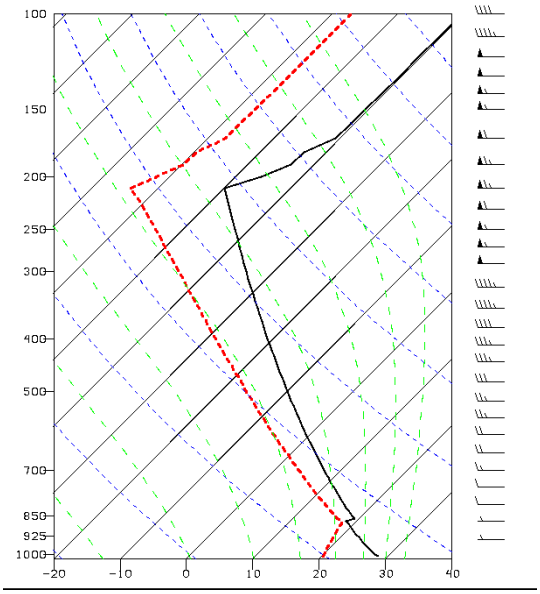

Figure 1. Skew-T diagram representing environmental sounding for idealized convective environment.

2.2. Idealized convective environment

In order to test the scheme for a controlled convective system in a homogeneous environment, we follow the method presented by Mahoney et al. (2009) for a "quasi-idealized" initial condition that is in thermal wind balance and that features westerly shear (Fig. 1). A 1.5-km deep warm bubble is embedded within this environment at the initial time in order to trigger convection in a specified location.

Owing to thermal wind balance, the environment features a meridional gradient of CAPE, with largest values at the southern edge of the domain of > 3000 J/kg, diminishing to ~1500 J/kg at the northern extent of the model domain. Westerly shear in the 0-6 km layer is roughly 30 kt in the center of the domain.

2.3. Model configuration

The control simulation uses the unaltered version of the KF CP scheme (Kain 2004) with WRF-ARW V2.2. The primary simulation domain features 12-km grid spacing. Simulations were performed with and without surface and radiation physics, but only those omitting these processes

are shown here. The Lin microphysics scheme was used along with TKE closure, but without a boundary layer scheme. Of course, the KF CP scheme was used.

Additional high-resolution domains, with grid lengths of 4 and 1.33 km, were run to allow comparisons of the results between runs with the parameterization packages and those with explicit convection (EC). In order to reduce noise and provide a more direct comparison with the 12-km simulations, output from the 1.33 km simulation is interpolated to a 12-km grid in some of the figures that follow; this output is labeled EC12.

3. RESULTS

The triggered convective system evolves over a period of several hours; simulations with parameterized convection produced mesoscale convective systems (MCSs) that were shorter lived relative to their high-resolution EC counterparts. Here, analyses will be shown for the 2 and 3 h time period, when the MCS had exhibited a sufficient influence on the surrounding environment. Analysis will focus on the zonal wind field in the immediate vicinity of the simulated convective system.

3.1. Convective system comparison

The total precipitation generated in the CTRL and CMT simulations shows strong similarity, with a leading region of convective precipitation and a trailing, westward-propagating line of convection associated with the cold pool that formed with the initial convective burst (Figs. 2a,b).

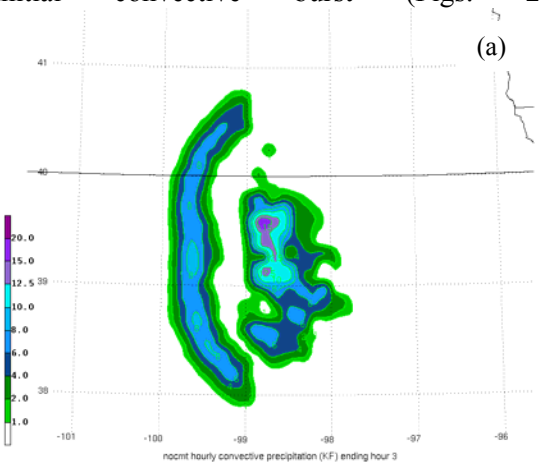

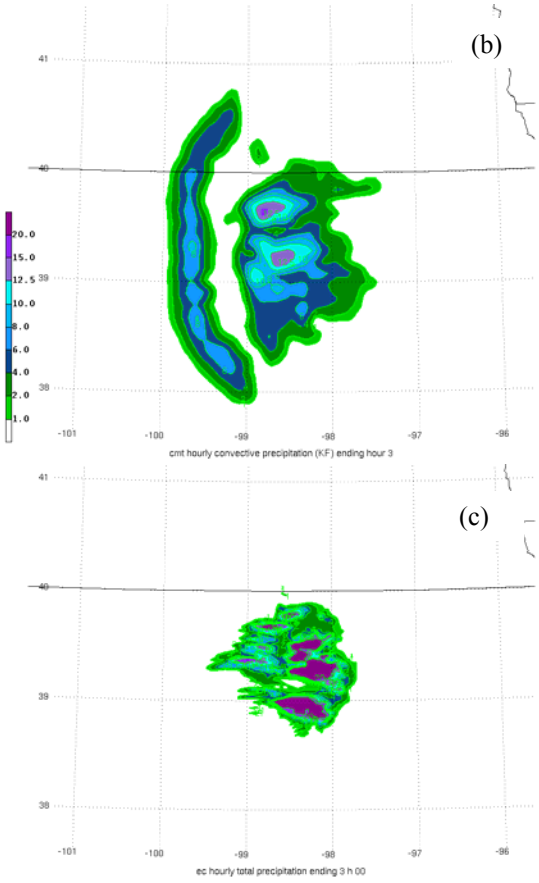

Fig. 2. Hourly precipitation (mm) ending hour 3 of the simulation: (a) NOCMT, (b) CMT, (c) EC 1.3 km.

The EC simulation does not include the westward-propagating convective feature, yet has a similar shape for the eastern MCS.

3.2. CMT modifications

The main focus of this investigation concerns the manner in which the convective system alters the horizontal wind field. In the control (NOCMT) simulation, an acceleration of the background westerly flow is found to the east of the convective system, and decelerated westerlies are found in the immediate vicinity of the convection (Fig. 3a). Comparisons were undertaken using data interpolated to isobaric surfaces, and are shown hwere for the 300-hPa level (Fig. 3).

The CMT simulation exhibits a similar pattern to that in the NOCMT run, but one that is considerably amplified relative to the control. The

difference is more pronounced in the weak flow region directly over the MCS. Comparison to the full-resolution EC 1.3 km simulation is hampered by the noise in the high-resolution data. Therefore, the output from the 1.3 km simulation is interpolated to the same 12-km grid used for the CMT and NOCMT simulations (Fig. 3c). This EC12 output exhibits an even more highly amplified version of the same flow anomalies seen in the CP runs.

It is encouraging that the runs with parameterized convection were able to reproduce the same general zonal wind anomaly pattern as found in the 1.3 km EC simulation, albeit much weaker in the NOCMT simulation and somewhat weaker in the CMT run. However, it is clear that the CMT simulation produces a result that is much closer to the EC wind field. This indicates that the inclusion of CMT has improved the representation of the convective zonal wind field adjustments in the vicinity of the simulated MCS.

Cross-sectional views of the full wind field are useful, but it was found to be more revealing to plot differences in the wind field between the start of the model run and hour 2. These east-west oriented sections thus show the net zonal wind tendency imparted by the convective system over the duration of the simulation to that point (Fig. 4).

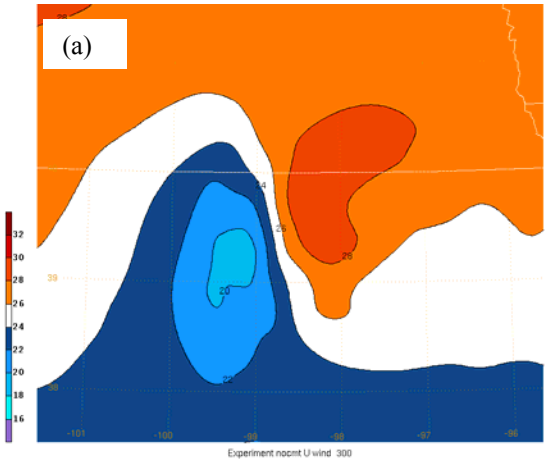

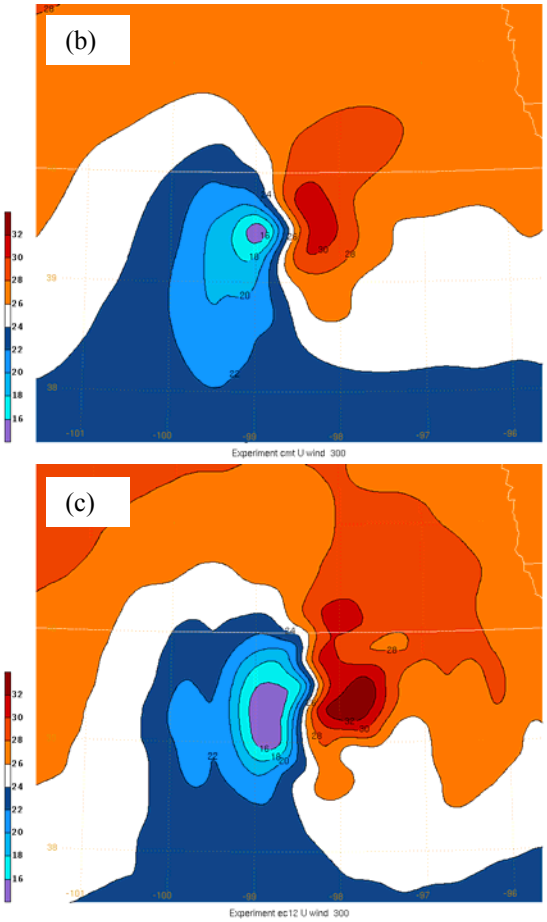

Fig. 3. As in Fig. 2, except for zonal wind (m/s) on an upper-tropospheric eta level corresponding roughly to the 250 hPa level.

The pattern of acceleration and deceleration seen in Fig. 3 is also evident in Fig. 4, and the results are consistent in that the CMT simulation produces a result that is closer to the EC run than does the NOCMT simulation. However, the EC cross section also reveals several features that are not present in the CMT simulation, including a region of westerly acceleration in the lower-middle troposphere to the west of the MCS, and accelerated westerly flow near the surface that appears to correspond to an outflow boundary (Fig. 4c). This latter feature is even more pronounced in full resolution EC data (not shown).

The lack of mid-level westerly acceleration in the CMT simulation may be due to a lack of account for the mesoscale pressure field in this version of the parameterization.

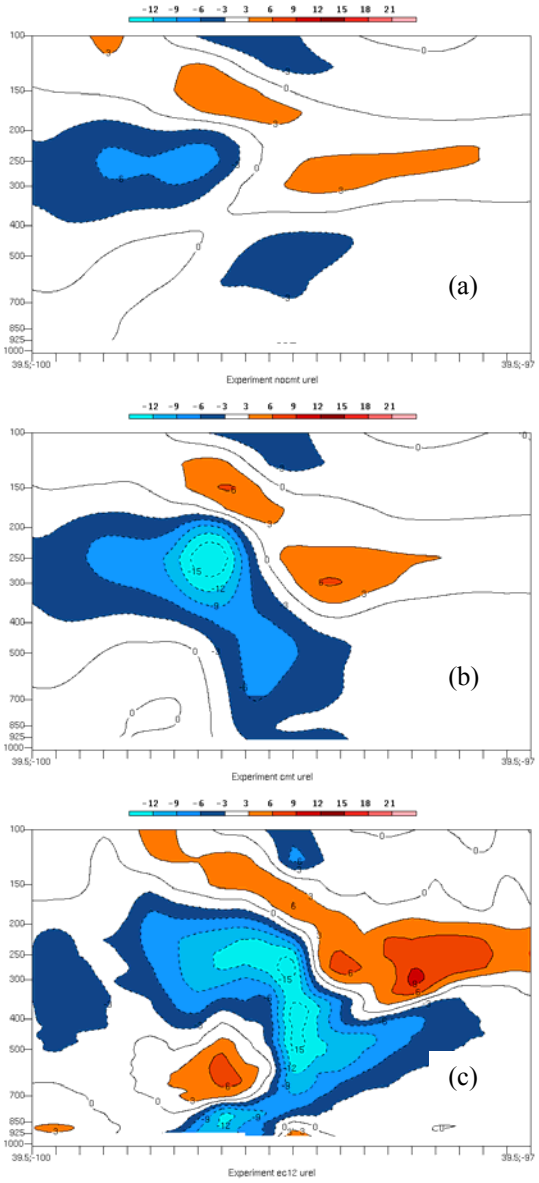

Fig. 4. Cross sections of difference between zonal wind field (m/s) at 2h minus that at the start of simulation.

In general, the CMT simulation appears most consistent with the interpolated EC simulation in the upper troposphere, especially in the vicinity of the zonal wind minimum. There is considerable difference between these simulations in lower and middle levels.

Cross-sectional differences between the NOCMT and CMT simulations (Fig. 5) quantifies the lack of deceleration aloft in the vicinity of the MCS in the NOCMT simulation, with a difference in excess of 10 m/s.

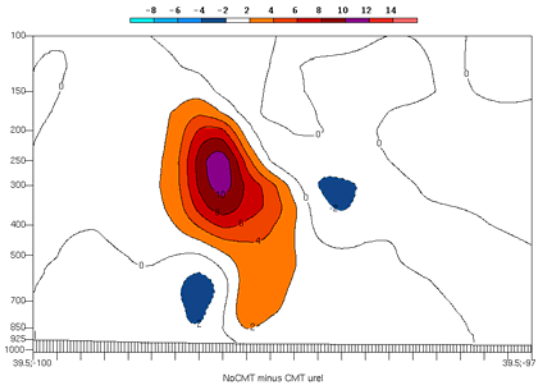

Fig. 5. Difference in zonal wind speed (m/s) at hour 2 for same cross section location as in Fig. 4.

The KF scheme works independently in each grid column, and local changes in the flow complicate the pattern of instantaneous convective momentum tendency. Nevertheless, a pattern that is somewhat spatially coherent is evident in this field (Fig. 6) due to the organized nature of the MCS.

Plots of two instantaneous momentum tendency isosurfaces, one positive and one negative, illustrate negative tendencies aloft with positive values beneath (Fig. 6). A vertical profile of the change at a selected point (Fig. 7) reveals strong negative tendencies just beneath the jet core.

Evidently, the local zonal flow acceleration to the east of the convective system arises from *grid-scale* pressure forces rather than from parameterized CMT, but the CMT is largely responsible for the upper-tropospheric deceleration of the flow located within and to the west of the MCS.

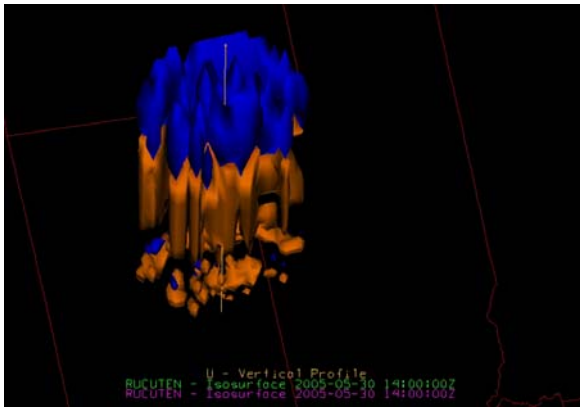

Fig. 6. Isosurfaces of coupled zonal momentum tendency parameterized by the KF CMT scheme. Cool (warm) colors represent decleration (acceleration).

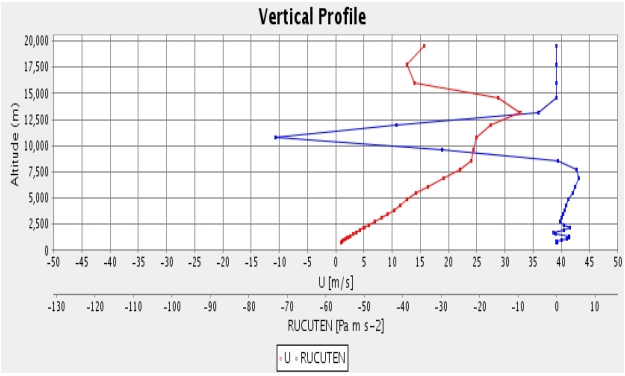

Fig. 7. Vertical profile of grid-relative u-wind (red) and parameterized coupled u-momentum tendency (blue). Location of profile shown by vertical yellow line in Fig. 7.

4. CONCLUSION AND FUTURE WORK

Parameterized convective momentum tendencies are sometimes omitted in mesoscale model simulations, yet this process is known to be important. Its neglect is more related to the complexity of its representation than to its magnitude. The role of this process has been established for global and general circulation models, but has received less attention for mesoscale models with grid lengths between 5 and 20 km. At these resolutions, organized convective systems can be partially resolved on the model grid.

Here, we have added convective momentum adjustment to the KF CP scheme in WRF-ARW. An idealized convective system is used to compare a control simulation, the CMT KF simulation, and a high-resolution EC simulation using the same initial conditions.

The main influence of convection is to decelerate the background flow in the immediate vicinity of convective updrafts, and provide westerly acceleration downstream of the convection. The westerly acceleration in this case arises from the development of high pressure aloft in response to latent heating, and this feature is resolved on the grid scale. The flow deceleration is due to the transport of lower momentum in the convective updraft, and in the CMT simulation, this process is represented by the parameterization scheme.

Results demonstrate that for this system, and for the grid lengths used (12 km), the CMT simulation more closely approaches the EC simulation (averaged to the same grid), especially for the deceleration seen in the upper troposphere. This suggests that a namelist option in WRF may be desirable for some simulations, although more testing is needed to explore the range of situations and grid lengths for which benefit is derived.

5. ACKNOWLEDGEMENTS

This research was supported by the NSF grant ATM-0603760, award to North Carolina State University. We wish to thank Ms. Megan Gentry for her work to modify WRF to pass generic momentum tendencies from the KF scheme to the solver. We thank Drs. Jack Kain (NSSL) and Brad Ferrier (EMC) for their encouragement to pursue this project.

6. REFERENCES

Flatau, M. and D. E. Stevens, 1987: The effect of horizontal pressure gradients on the momentum transport in tropical convective lines. Part I: The results of the convective parameterization. *J. Atmos. Sci.*, **44**, 2074–2087.

Fritsch, J. M., and C. F. Chappel, 1980a: Numerical prediction of convectively driven mesoscale pressure systems. Part I: Convective parameterization. *J. Atmos. Sci.*, **27**, 1722–1733.

Fritsch, J. M., and C. F. Chappel, 1980b: Numerical prediction of convectively driven mesoscale pressure systems. Part II: Mesoscale model. *J. Atmos. Sci.*, **27**, 1734–1762.

Gregory, D. R. Kershaw, and P. M. Inness, 1997: Parametrization of momentum transport by convection. II: Tests in single-column and general circulation models. *Q. J. R. Meteorol. Soc.*, **123**, 1153–1183.

Grubisic, V. and M. W. Moncrieff, 2000: Parameterization of convective momentum transport in highly baroclinic conditions. . *J. Atmos. Sci.*, **57**, 3035–3049.

Kain, J. S., 2004: The Kain–Fritsch convective parameterization: An update. *J. Appl. Meteor.*, **43**, 170–181.

Kain, J. S., and J. M. Fritsch, 1990: Convective parameterization for mesoscale models: The Kain-Fritsch scheme. Meteor. Monogr.: The Representation of Cumulus Convection in Numerical Models, AMS, Emanuel and Raymond, Eds.

Kershaw and Gregory 1997: Parametrization of momentum transports by convection. **I:** Theory and cloud modelling results. *Q. J. R. Meteorol.* Soc.**, 123,** 1133–1151.

Kim, D., J.-S. Kug, I.-S. Kang, F.-F. Jin and A. T. Wittenberg, 2008: Tropical Pacific impacts of convective momentum transport in the SNU coupled GCM. *Clim. Dyn.* **31**, 213–226.

Han, J. and H.-L.Pan, 2005: Sensitivity of hurricane intensity forecast to convective momentum transport parameterization. *Mon. Wea. Rev.*, **134**, 664–674.

LeMone, M. A., 1983: Momentum transport by a line of cumulonimbus. *J. Atmos. Sci.***, 40,** 1815–1834.

Mahoney et al. 2009: The role of momentum transport in the motion of a quasi-idealized mesoscale convective system. *Mon. Wea. Rev.*, **137**, 3316–3338.

Mapes, B. E., and X. Wu, 2001: Convective eddy momentum tendencies in long cloud-resolving model simulations. *J. Atmos. Sci.,* **58,** 517–526.

Mechem, D. B., S. S. Chen, and R. A. Houze, Jr., 2006: Momentum transport processes in the stratiform regions of mesoscale convective systems over the western Pacific warm pool. *Quart. J. Roy. Meteor. Soc.*, **132**, 709–736.

Moncrieff, M. W., 1981: A theory of organized steady convection and its transport properties. *Q. J. R. Meteorol. Soc.*, **107**, 29–50.

Moncrieff, M. W., and C. Liu, 2006: Representing convective organization in prediction models by a hybrid strategy. *J. Atmos. Sci.,* **63**, 3404–3420.

Wu, X. Q., X. Z. Liang, and G. J. Zhang 2003: Seasonal migration of ITCZ precipitation across the equator: Why can't GCMs simulate it? *Geophys. Res. Lett.*, **30**, 1824–1828.

Wu, X. Q., and M. Yanai, 1994: Effects of vertical wind shear on the cumulus transport of momentum: Observations and parametrization. *J. Atmos. Sci.***, 51,** 1640–1660.

Zhang, G. J., and N. A. McFarlane, 1995: Role of convective scale momentum transport in climate simulation. *J. Geophys. Res.*, **100**, 1417–1426.